Journal of Applied Mechanics and Technical Physics, Vol. 47, No. 4, pp. 556–563, 2006

EFFECT OF SCATTERING OF ELASTIC HARMONIC WAVES IN THE FAR ZONE BY A SPATIAL CRACK

V. V. Mykhas'kiv,[1] N. D. Grilitskii,[2] and I. O. Butrak[1]

UDC 539.3

A three-dimensional wave field formed owing to diffraction of low-frequency waves on a curved crack in an infinite elastic solid at a large distance from the defect is studied by the method of boundary integral equations. Direction diagrams of the scattered field versus the excentricity of the crack surface and wavenumber are obtained for different directions of incidence of planar longitudinal waves onto a gently sloping spheroidal crack.

Key words: *elastic solid, spatial crack, harmonic wave, scattered field, direction diagram, method of boundary integral equations.*

Introduction. In solving problems of seismic science, diagnostics, and nondestructive evaluation, much attention is paid to studying the interaction of elastic waves with defects, such as cracks, which have a sophisticated geometry in reality. The defect topology significantly affects the wave pattern both in the vicinity of the scatterer and far from the latter. An analysis of the near zone, in particular, dynamic coefficients of stress intensity in three-dimensional solids with cracks of various configurations was performed in [1–7] by the method of boundary integral equations (BIE). In the present paper, this method is used to study the far elastic wave field on the basis of dependences between its amplitude–frequency characteristics and the boundary functions of opening of a defect of an arbitrary shape (BIE solutions). It should be noted that a similar approach was used previously to solve three-dimensional problems of diffraction of acoustic and electromagnetic waves on curved surfaces [8, 9] and of elastic waves on planar cracks without [10, 11] and with [12, 13] allowance for their interaction.

Formulation of the Problem in the Form of Integral Equations and Relations. Let an elastic harmonic wave propagate in an infinite elastic solid with a crack aligned with an arbitrary smooth surface S. The components of displacements and corresponding stresses are

$$u_j^{\rm int}(\boldsymbol{x},t)=u_j^{\rm int}(\boldsymbol{x})\exp(-i\omega t)\qquad (j=\overline{1,3}),$$
$$\sigma_{jr}^{\rm int}(\boldsymbol{x},t)=\sigma_{jr}^{\rm int}(\boldsymbol{x})\exp(-i\omega t)\qquad (j,r=\overline{1,3}),\tag{1}$$

where $\boldsymbol{x}(x_1,x_2,x_3)$ is the radius vector of the point of the solid, t is the time, $i=\sqrt{-1}$, $u_j^{\rm int}(\boldsymbol{x})$ and $\sigma_{jr}^{\rm int}(\boldsymbol{x})$ $(j,r=\overline{1,3})$ are the amplitudes of displacements and stresses of the incident wave, respectively, and ω is the cyclic frequency. The crack surfaces are free from forces (Fig. 1).

In a steady process, the exponential time factor in Eq. (1) can be omitted. Then, the diffraction field of displacements u_j^* in the solid induced by wave–crack interaction can be presented as the superposition [4]

$$u_j^*(\boldsymbol{x})=u_j^{\rm int}(\boldsymbol{x})+u_j(\boldsymbol{x}),\qquad j=\overline{1,3},\tag{2}$$

[1]Podstrigach Institute of Applied Problems in Mechanics and Mathematics, National Academy of Sciences of Ukraine, L'viv 79060, Ukraine. [2]L'viv Department of the Dnepropetrovsk National University of Railroad Transport, L'viv 79052, Ukraine; tex@iapmm.lviv.ua. Translated from Prikladnaya Mekhanika i Tekhnicheskaya Fizika, Vol. 47, No. 4, pp. 115–123, July–August, 2006. Original article submitted May 4, 2005.

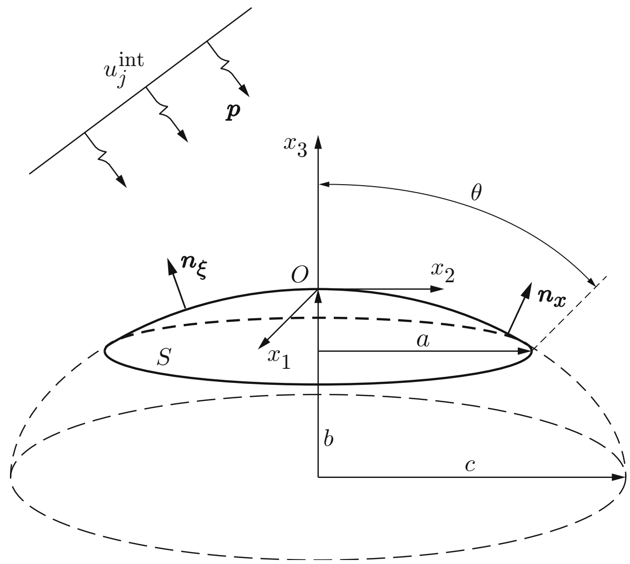

Fig. 1. Geometry of the problem.

where $\boldsymbol{u}(u_1, u_2, u_3)$ are the unknown displacements of the wave reflected from the defect, which satisfy the conditions of emission at infinity and the diffraction equations of motion in the case of steady oscillations:

$$\omega_1^{-2}\nabla(\nabla\cdot\boldsymbol{u}) - \omega_2^{-2}\nabla\times(\nabla\times\boldsymbol{u}) + \boldsymbol{u} = 0, \tag{3}$$

$\omega_j = \omega/c_j$ $(j = 1, 2)$ are the wavenumbers, c_1 and c_2 are the velocities of propagation of longitudinal and transverse waves, respectively, and ∇ is a three-dimensional nabla-operator.

The potential theory being used, the solution of problem (1)–(3) is reduced to the solution of the following system of three BIEs with respect to the jumps of displacements of the opposite surfaces of the crack Δu_j $(j = \overline{1,3})$ in the direction of the coordinate axes [14]:

$$\sum_{r=1}^{3}\iint\limits_S \Delta u_r(\boldsymbol{\xi},\omega)\Omega_{jr}(\boldsymbol{x},\boldsymbol{\xi},\omega)\,dS_{\boldsymbol{\xi}} = -\frac{1}{4G}\sum_{r=1}^{3}\sigma_{jr}^{\text{int}}(\boldsymbol{x},\omega)n_{r\boldsymbol{x}}, \qquad j=\overline{1,3}, \quad \boldsymbol{x}\in S. \tag{4}$$

Here the right sides describe the forces (with the opposite sign) caused by the incident wave in the region of the defect, the kernels Ω_{jr} have a singularity of the Helmholtz potential

$$\Omega_{jr}(\boldsymbol{x},\boldsymbol{\xi},\omega) = \Big(\frac{1-2\gamma^2}{2}\sum_{m=1}^{3}\sum_{p=1}^{3}(\delta_{jm}n_{p\boldsymbol{x}}n_{r\boldsymbol{\xi}} + \delta_{rm}n_{j\boldsymbol{x}}n_{p\boldsymbol{\xi}})\frac{\partial^2}{\partial x_m\,\partial x_p}$$

$$-\frac{(1-2\gamma^2)^2}{4}\omega_2^2 n_{j\boldsymbol{x}}n_{r\boldsymbol{\xi}}\Big)\frac{\exp(i\omega_1|\boldsymbol{x}-\boldsymbol{\xi}|)}{|\boldsymbol{x}-\boldsymbol{\xi}|} + \frac{1}{4}\sum_{m=1}^{3}\sum_{p=1}^{3}\Big[\delta_{jr}n_{p\boldsymbol{x}}n_{m\boldsymbol{\xi}} + \delta_{jp}n_{r\boldsymbol{x}}n_{m\boldsymbol{\xi}}$$

$$+\delta_{rm}n_{p\boldsymbol{x}}n_{j\boldsymbol{\xi}} + \delta_{mj}\delta_{pr}(\boldsymbol{n_x}\cdot\boldsymbol{n_\xi})\Big]\frac{\partial^2}{\partial x_m\,\partial x_p}\Big(\frac{\exp(i\omega_2|\boldsymbol{x}-\boldsymbol{\xi}|)}{|\boldsymbol{x}-\boldsymbol{\xi}|}\Big)$$

$$+\frac{1}{\omega_2^2}\frac{\partial^2}{\partial x_j\,\partial x_r}\sum_{m=1}^{3}\sum_{p=1}^{3}n_{m\boldsymbol{x}}n_{p\boldsymbol{\xi}}\frac{\partial^2}{\partial x_m\,\partial x_p}\Big(\frac{\exp(i\omega_2|\boldsymbol{x}-\boldsymbol{\xi}|)-\exp(i\omega_1|\boldsymbol{x}-\boldsymbol{\xi}|)}{|\boldsymbol{x}-\boldsymbol{\xi}|}\Big),$$

G is the shear modulus, $\gamma = c_2/c_1 = \sqrt{(1-2\nu)/(2(1-\nu))}$, ν is Poisson's ratio, δ_{jr} is the Kronecker symbol, $|\boldsymbol{x}-\boldsymbol{\xi}|$ is the distance between the point of the field $\boldsymbol{x}(x_1,x_2,x_3)$ and the point of integration $\boldsymbol{\xi}(\xi_1,\xi_2,\xi_3)$, and $n_{p\boldsymbol{x}}$ and $n_{p\boldsymbol{\xi}}$ $(p=\overline{1,3})$ are the projections of the normal to the surface S at these points.

At large distances from the crack $|\boldsymbol{x}| \gg |\boldsymbol{\xi}|$ ($\boldsymbol{\xi} \in S$), asymptotic presentations of displacements of the scattered waves are valid [7], which are written in the following form in the spherical coordinate system $x_1 = R\sin\varphi\cos\psi$, $x_2 = R\sin\varphi\sin\psi$, $x_3 = R\cos\varphi$:

$$u_R(R,\varphi,\psi) = \frac{\exp(i\omega_1 R)}{R} F_P(\varphi,\psi), \qquad R \to \infty,$$

$$u_\varphi(R,\varphi,\psi) = \frac{\exp(i\omega_2 R)}{R} F_{SV}(\varphi,\psi), \qquad R \to \infty, \tag{5}$$

$$u_\psi(R,\varphi,\psi) = \frac{\exp(i\omega_2 R)}{R} F_{SH}(\varphi,\psi), \qquad R \to \infty.$$

In formulas (5), the amplitudes of the planar longitudinal wave F_P and those of vertically (F_{SV}) and horizontally (F_{SH}) polarized planar transverse waves have an integral dependence on the functions Δu_j ($j = \overline{1,3}$):

$$F_P(\varphi,\psi) = i\omega_1 \sum_{j=1}^{3}\sum_{s=1}^{3} \Big[2\gamma^2 \tilde{x}_j\tilde{x}_s + (1-2\gamma^2)\delta_{js}\Big] \iint\limits_S \exp(-i\omega_1(\tilde{\boldsymbol{x}}\cdot\boldsymbol{\xi}))\Delta u_j(\boldsymbol{\xi}) n_{s\boldsymbol{\xi}}\, dS_{\boldsymbol{\xi}},$$

$$F_{SV}(\varphi,\psi) = i\omega_2 \sum_{j=1}^{3}\sum_{s=1}^{3} \Big[\tilde{v}_j\tilde{x}_s + \tilde{v}_s\tilde{x}_j\Big] \iint\limits_S \exp(-i\omega_2(\tilde{\boldsymbol{x}}\cdot\boldsymbol{\xi}))\Delta u_j(\boldsymbol{\xi}) n_{s\boldsymbol{\xi}}\, dS_{\boldsymbol{\xi}}, \tag{6}$$

$$F_{SH}(\varphi,\psi) = i\omega_2 \sum_{j=1}^{3}\sum_{s=1}^{3} \Big[\tilde{h}_j\tilde{x}_s + \tilde{h}_s\tilde{x}_j\Big] \iint\limits_S \exp(-i\omega_2(\tilde{\boldsymbol{x}}\cdot\boldsymbol{\xi}))\Delta u_j(\boldsymbol{\xi}) n_{s\boldsymbol{\xi}}\, dS_{\boldsymbol{\xi}}.$$

Here $\tilde{\boldsymbol{x}}$, $\tilde{\boldsymbol{v}}$, and $\tilde{\boldsymbol{h}}$ are the unit vectors:

$$\tilde{\boldsymbol{x}} = \begin{bmatrix} \sin\varphi\cos\psi \\ \sin\varphi\sin\psi \\ \cos\varphi \end{bmatrix}, \qquad \tilde{\boldsymbol{v}} = \begin{bmatrix} \cos\varphi\cos\psi \\ \cos\varphi\sin\psi \\ -\sin\varphi \end{bmatrix}, \qquad \tilde{\boldsymbol{h}} = \begin{bmatrix} -\sin\psi \\ \cos\psi \\ 0 \end{bmatrix}.$$

Thus, the solution of the problem of wave scattering in the far zone by a spatial crack reduces to determining the functions of dynamic opening of the defect in BIEs (4) with their subsequent substitution into the integral relations (6).

Construction of the Solution in the Long-Wave Approximation for a Gently Sloping Crack. To obtain a particular solution of the problem, we consider an elastic solid with a spheroidal crack with the surface $x_3 = F(x_1,x_2) = b\Big(\sqrt{1-(x_1^2+x_2^2)/c^2} - 1\Big)$ in the coordinate system whose origin is located at the defect apex (b and c are the semi-axes of the ellipsoid of revolution; $b \leqslant c$). The crack contour is formed by the line of intersection of the ellipsoid of revolution with a plane parallel to the coordinate plane x_1Ox_2; this is a circle of radius a (see Fig. 1). The geometric parameters of the crack are chosen from the condition that the crack is gently sloping, i.e., the angle between the normals at arbitrary points of the surface S should not be greater than $\pi/4$. A planar longitudinal wave in the direction of the orth $\boldsymbol{p}(p_1,p_2,p_3)$ is incident onto the crack. The stress components of the wave are

$$\sigma_{jr}^{\text{int}}(\boldsymbol{x},\omega) = P_0[2\gamma^2 p_r p_j + (1-2\gamma^2)\delta_{jr}]\exp(i\omega_1(\boldsymbol{p}\cdot\boldsymbol{x})), \qquad j,r = \overline{1,3},$$

where P_0 is a constant corresponding to the amplitude of normal forces in the planes parallel to the wave front.

The assumptions made on the gentle slope of the crack and on the character of the steady excitation allow us to solve BIEs (4) by the method of the small parameter on the basis of the presentations

$$\exp(i\omega_j r) = \sum_{k=0}^{\infty} \frac{(i\omega_j r)^k}{k!}, \qquad j = 1,2, \quad r = |\boldsymbol{x}-\boldsymbol{\xi}| \quad \text{or} \quad r = \boldsymbol{p}\cdot\boldsymbol{x},$$

$$F(x_1,x_2) = -\sum_{q=0}^{\infty} \frac{(2q-3)!!}{2q!!}\Big(\frac{x_1^2+x_2^2}{a^2}\Big)^q \varepsilon^{2q}, \qquad (x_1,x_2) \in S_0, \tag{7}$$

where $\varepsilon = a/c < 1$ is the geometric parameter and S_0 is the circular region of radius a, which is the projection of the region S onto the coordinate plane x_1Ox_2.

Presentations (7) allow us to expand the kernels and the right sides of BIEs (4) into converging double series in terms of the frequency and geometric parameters. Using similar expansions for the sought functions in the form

$$\Delta u_j(\boldsymbol{x}, \omega) = \sum_{q=0}^{\infty}\sum_{k=0}^{\infty} \Delta u_j^{(k,q)}(x_1, x_2)(i\omega_2)^k \varepsilon^q \qquad (j = \overline{1,3}) \tag{8}$$

and equating expressions with identical orders of the small parameters in the right and left sides of Eqs. (4), we find integral equations, which are recurrent with respect to the superscripts k and q, over a planar region S_0 with a static (Newton) kernel for determining the functions $\Delta u_j^{(k,q)}$ ($j = \overline{1,3}$; $k, q = \overline{0,\infty}$). These equations admit an analytical solution on the basis of the theorem about their polynomial persistence [15]. In particular, if the direction of the generating wave coincides with the direction of the orth $\boldsymbol{p} = \boldsymbol{p}(0,0,-1)$ (direction I) or with the direction of the orth $\boldsymbol{p} = \boldsymbol{p}(0,0,1)$ (direction II), the approximate solutions of BIEs (4) with retained terms of the order of $(i\omega_2)^3\varepsilon$ and $(i\omega_2)\varepsilon^2$ are obtained for the following values of coefficients in Eq. (8):

$$\Delta u_j^{(0,0)}(\boldsymbol{x}) = 0 \quad (j = 1,2), \qquad \Delta u_3^{(0,0)}(\boldsymbol{x}) = -\frac{P_0}{2G(1-\gamma^2)\pi^2}\sqrt{a^2 - x_1^2 - x_2^2},$$

$$\Delta u_j^{(0,1)}(\boldsymbol{x}) = -\frac{P_0}{12G\pi^2}\,\frac{3 - 9\gamma^2 + 8\gamma^4}{(1-\gamma^2)^2}\,\frac{b}{c}\,\frac{x_j}{a}\sqrt{a^2 - x_1^2 - x_2^2} \qquad (j = 1,2),$$

$$\Delta u_3^{(0,1)}(\boldsymbol{x}) = 0, \qquad \Delta u_j^{(0,2)}(\boldsymbol{x}) = 0 \qquad (j = 1,2),$$

$$\Delta u_3^{(0,2)}(\boldsymbol{x}) = \frac{P_0}{144G\pi^2}\,\frac{1}{(1-\gamma^2)^3}\left(\frac{b}{c}\right)^2\frac{1}{a^2}\sqrt{a^2 - x_1^2 - x_2^2}$$

$$\times\Big[2(9 - 30\gamma^2 + 41\gamma^4 - 24\gamma^6)a^2 - (9 - 42\gamma^2 + 73\gamma^4 - 48\gamma^6)(x_1^2 + x_2^2)\Big],$$

$$\Delta u_j^{(1,q)}(\boldsymbol{x}) = 0 \quad (j = \overline{1,3},\ q = 0,1), \qquad \Delta u_j^{(1,2)}(\boldsymbol{x}) = 0 \quad (j = 1,2),$$

$$\Delta u_3^{(1,2)}(\boldsymbol{x}) = \mp\frac{P_0 b}{18G\pi^2}\,\frac{\gamma}{1-\gamma^2}\,\frac{1}{a^2}\sqrt{a^2 - x_1^2 - x_2^2}\,(a^2 + 2(x_1^2 + x_2^2)), \tag{9}$$

$$\Delta u_j^{(2,0)}(\boldsymbol{x}) = 0 \qquad (j = 1,2),$$

$$\Delta u_3^{(2,0)}(\boldsymbol{x}) = \frac{P_0}{72G\pi^2}\,\frac{3 - 4\gamma^2 + 3\gamma^4}{(1-\gamma^2)^2}\,(4a^2 - x_1^2 - x_2^2)\sqrt{a^2 - x_1^2 - x_2^2},$$

$$\Delta u_j^{(2,1)}(\boldsymbol{x}) = \frac{P_0}{720G\pi^2}\,\frac{1}{(1-\gamma^2)^3}\,\frac{b}{c}\,\frac{x_j}{a}\sqrt{a^2 - x_1^2 - x_2^2}\,\Big[(27 - 86\gamma^2 + 105\gamma^4 - 28\gamma^6 + 16\gamma^8)a^2$$

$$- (21 - 53\gamma^2 + 55\gamma^4 - 19\gamma^6 + 8\gamma^8)(x_1^2 + x_2^2)\Big] \qquad (j = 1,2),$$

$$\Delta u_3^{(2,1)}(\boldsymbol{x}) = 0, \qquad \Delta u_j^{(3,0)}(\boldsymbol{x}) = 0 \qquad (j = 1,2),$$

$$\Delta u_3^{(3,0)}(\boldsymbol{x}) = \frac{P_0 a^3}{90G\pi^3}\,\frac{8 + 15\gamma - 40\gamma^3 + 32\gamma^5}{(1-\gamma^2)^2}\sqrt{a^2 - x_1^2 - x_2^2}, \qquad \Delta u_3^{(3,1)}(\boldsymbol{x}) = 0,$$

$$\Delta u_j^{(3,1)}(\boldsymbol{x}) = \frac{P_0 a^2}{270G\pi^3}\,\frac{b}{c}\,x_j\,\frac{48\gamma^7 - 24\gamma^5 + 25\gamma^3 + 32\gamma^2 + 15\gamma - 16}{(1-\gamma^2)^3}\sqrt{a^2 - x_1^2 - x_2^2} \quad (j = 1,2).$$

Hereinafter, in the signs "$\mp$" and "$\pm$", the upper and lower signs refer to direction I and direction II, respectively.

For a further study of dynamic displacements in the far zone, it is necessary to calculate integrals (6) with allowance for the function of defect opening (8), (9). Using the asymptotic formulas (7) with $r = \tilde{\boldsymbol{x}} \cdot \boldsymbol{\xi}$ and the method of reduction of surface integrals to double integrals of the form

$$\iint\limits_{S_0} \sqrt{a^2 - \xi_1^2 - \xi_2^2}\, dS_{\boldsymbol{\xi}} = \frac{2}{3}\pi a^3, \qquad \iint\limits_{S_0} \xi_j \sqrt{a^2 - \xi_1^2 - \xi_2^2}\, dS_{\boldsymbol{\xi}} = 0 \qquad (j = 1, 2),$$

$$\iint\limits_{S_0} \xi_1\xi_2 \sqrt{a^2 - \xi_1^2 - \xi_2^2}\, dS_{\boldsymbol{\xi}} = 0, \qquad \iint\limits_{S_0} \xi_j^2 \sqrt{a^2 - \xi_1^2 - \xi_2^2}\, dS_{\boldsymbol{\xi}} = \frac{2}{15}\pi a^5 \qquad (j = 1, 2),$$

$$\iint\limits_{S_0} \xi_i^2\xi_j \sqrt{a^2 - \xi_1^2 - \xi_2^2}\, dS_{\boldsymbol{\xi}} = 0 \qquad (i, j = 1, 2),$$

$$\iint\limits_{S_0} \xi_j^4 \sqrt{a^2 - \xi_1^2 - \xi_2^2}\, dS_{\boldsymbol{\xi}} = \frac{2}{35}\pi a^7 \quad (j = 1, 2), \qquad \iint\limits_{S_0} \xi_1^2\xi_2^2 \sqrt{a^2 - \xi_1^2 - \xi_2^2}\, dS_{\boldsymbol{\xi}} = \frac{2}{105}\pi a^7,$$

$$\iint\limits_{S_0} \xi_i^3\xi_j \sqrt{a^2 - \xi_1^2 - \xi_2^2}\, dS_{\boldsymbol{\xi}} = 0 \qquad (i, j = 1, 2, \quad i \neq j),$$

for the two methods of crack entrainment into the wave field, we obtain the following approximations of the amplitudes of scattering of waves of different modes:

$$\begin{aligned} F_P(\varphi) = i\chi F_* \Big\langle g_1 + g_2 \cos^2\varphi + (g_3 + g_4 \sin^2\varphi + g_5 \cos^2\varphi)\Big(\frac{b}{c}\Big)^2 \frac{\sin^2\theta}{1 - k^2\cos^2\theta} \\ + i[g_6 \sin^2\varphi\cos\varphi + (g_7 + g_8\cos^2\varphi)(\cos\varphi \pm 1)]\, \frac{b}{c}\, \frac{\sin\theta}{\sqrt{1 - k^2\cos^2\theta}}\, \chi \\ - (g_9 + g_{10}\sin^2\varphi + g_{11}\sin^2 2\varphi + g_{12}\cos^2\varphi)\chi^2 \\ - i\Big(g_{13} + g_{14}\cos^2\varphi + (g_{15} + g_{16}\sin^2\varphi)\sin^2\varphi\cos\varphi\, \frac{b}{c}\, \frac{\sin\theta}{\sqrt{1 - k^2\cos^2\theta}}\Big)\chi^3\Big\rangle, \end{aligned} \tag{10}$$

$$\begin{aligned} F_{SV}(\varphi) = i\chi\, \frac{F_*}{\gamma} \Big\langle \sin 2\varphi + h_1 \sin 2\varphi \Big(\frac{b}{c}\Big)^2 \frac{\sin^2\theta}{1 - k^2\cos^2\theta} \\ + i(h_2 \sin\varphi\cos 2\varphi + h_3\cos\varphi\sin 2\varphi \pm h_4 \sin 2\varphi)\frac{b}{c}\, \frac{\sin\theta}{\sqrt{1 - k^2\cos^2\theta}}\, \chi - (h_5 + h_6\sin^2\varphi)\sin 2\varphi\chi^2 \\ - i\Big(h_7 \sin 2\varphi + (h_8 + h_9 \sin^2\varphi)\cos 2\varphi \sin\varphi\, \frac{b}{c}\, \frac{\sin\theta}{\sqrt{1 - k^2\cos^2\theta}}\Big)\chi^3\Big\rangle; \end{aligned}$$

$$F_{SH}(\varphi) = 0 \tag{11}$$

[relation (11) is valid for both direction I and direction II]. In Eqs. (10) and (11), $\chi = \omega_2 a$ is the normalized wavenumber, θ is the angle between the normal to the crack surface on its contour and the Ox_3 axis, which characterizes the degree of crack curvature (see Fig. 1), $\cos^2\theta = (1 - (a/c)^2)/(1 - k^2(a/c)^2)$, $k^2 = 1 - (b/c)^2$, $F_* = P_0 a^2\gamma/(3G\pi(1 - \gamma^2))$ is a normalization quantity proportional to the crack-base area, and

$$g_1 = 2\gamma^2 - 1, \qquad g_2 = -2\gamma^2, \qquad g_3 = \frac{\gamma^2(1 - 2\gamma^2)(3 - 6\gamma^2 + 2\gamma^4)}{15(1 - \gamma^2)^2},$$

$$g_4 = -\frac{\gamma^2(3 - 9\gamma^2 + 8\gamma^4)}{15(1 - \gamma^2)}, \qquad g_5 = \frac{2\gamma^2(3 - 9\gamma^2 + 11\gamma^4 - 6\gamma^6)}{15(1 - \gamma^2)^2}, \qquad g_6 = \frac{\gamma^3(9 - 15\gamma^2 + 8\gamma^4)}{60(1 - \gamma^2)},$$

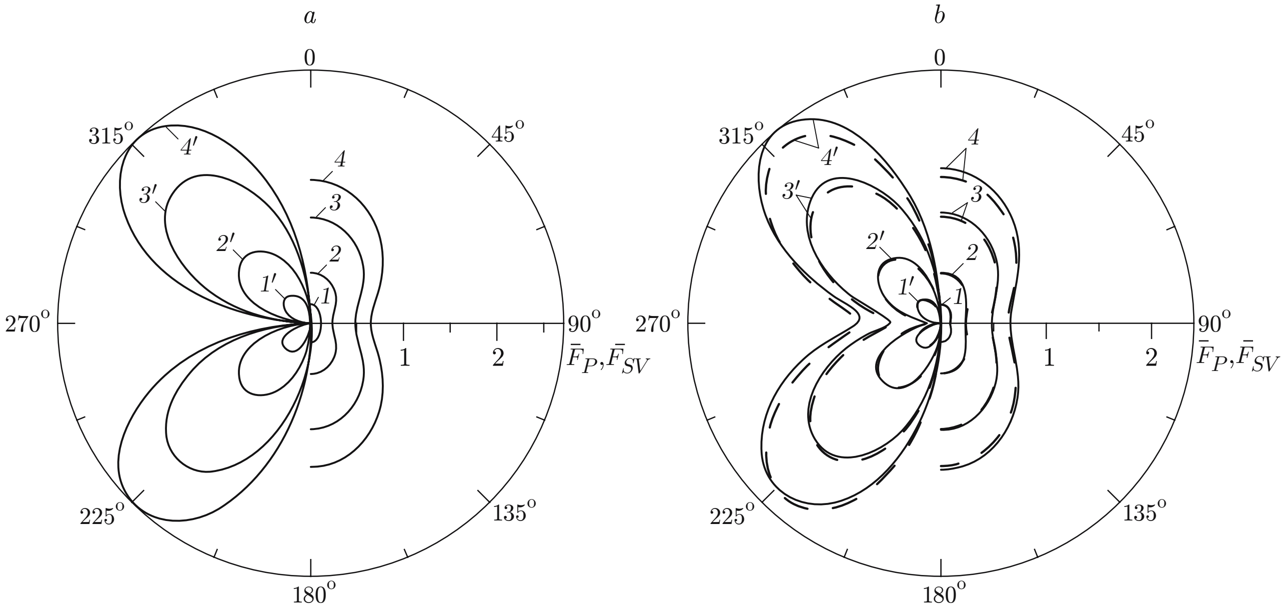

Fig. 2. Direction diagrams of the scattered field produced by a planar crack with $\theta = 0$ (a) and by a curved spheroidal crack with $\theta = 40°$ (b): curves 1–4 and 1′–4′ show the characteristics of the longitudinal and transverse reflected waves, respectively, for $\chi = 0.2$ (1 and 1′) 0.5 (2 and 2′), 0.9 (3 and 3′), and 1.1 (4 and 4′); the solid and dashed curves refer to propagation of the generating wave in direction I and direction II, respectively.

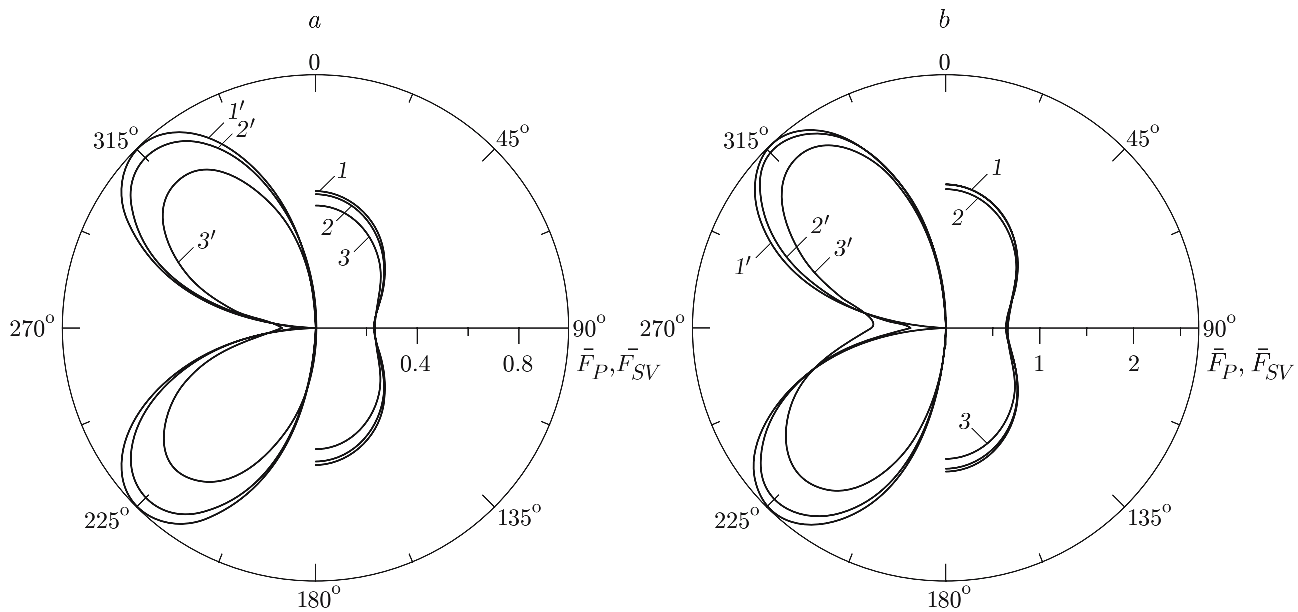

Fig. 3. Direction diagrams of the scattered field produced by a crack for the wave incident in direction I for $\chi = 0.5$ (a) and 1.1 (b); curves 1–3 and 1′–3′ show the characteristics of the longitudinal and transverse reflected waves, respectively; planar crack with $\theta = 0$ (1 and 1′); spherical crack with $\theta = 30°$ (2 and 2′); spheroidal crack with $\theta = 40°$ (3 and 3′).

$$g_7 = -\frac{\gamma(1-2\gamma^2)}{5}, \qquad g_8 = -\frac{2\gamma^3}{5}, \qquad g_9 = \frac{(1-2\gamma^2)(3-4\gamma^2+3\gamma^4)}{10(1-\gamma^2)}, \qquad g_{10} = \frac{\gamma}{2}\, g_7,$$

$$g_{11} = \frac{\gamma}{8}\, g_8, \qquad g_{12} = \frac{\gamma^2(3-4\gamma^2+3\gamma^4)}{5(1-\gamma^2)}, \qquad g_{13} = \frac{(1-2\gamma^2)(8+15\gamma-40\gamma^3+32\gamma^5)}{45(1-\gamma^2)\pi},$$

$$g_{14} = \frac{2\gamma^2(8+15\gamma-40\gamma^3+32\gamma^5)}{45(1-\gamma^2)\pi}, \qquad g_{15} = -\frac{\gamma^3(165-414\gamma^2+439\gamma^4-168\gamma^6+16\gamma^8)}{1260(1-\gamma^2)^2},$$

$$g_{16} = \frac{\gamma^5(9-15\gamma^2+8\gamma^4)}{210(1-\gamma^2)},$$

$$h_1 = -\frac{9-30\gamma^2+39\gamma^4-20\gamma^6}{30(1-\gamma^2)^2}, \qquad h_2 = \frac{2}{\gamma^3}\, g_6, \qquad h_3 = \frac{1}{5}, \qquad h_4 = \gamma h_3,$$

$$h_5 = -\frac{g_9}{1-2\gamma^2}, \qquad h_6 = \frac{h_3}{2}, \qquad h_7 = -\frac{8+15\gamma-40\gamma^3+32\gamma^5}{45(1-\gamma^2)\pi},$$

$$h_8 = -\frac{165-270\gamma^2+247\gamma^4-24\gamma^6+16\gamma^8}{2520(1-\gamma^2)^2}, \qquad h_9 = \frac{9-15\gamma^2+8\gamma^4}{420(1-\gamma^2)}.$$

It should be noted that the identical distribution of the amplitudes of scattering of longitudinal and vertically polarized transverse waves in the meridional planes $\psi = \text{const}$ and also the zero amplitudes of scattering of horizontally polarized transverse waves is caused by the symmetry of the crack surface and the generating steady expansion–compression wave with respect to the Ox_3 axis.

Analysis of Direction Diagrams of the Scattered Field. The dimensionless amplitudes $\bar{F}_A(\varphi) = |F_A(\varphi)|/F_*$ $(A \equiv P,\ SV)$ as functions of the angular coordinate φ plotted in Figs. 2 and 3 were calculated for a spheroidal crack with a contour radius $a = 0.5c$ for Poisson's ratio $\nu = 0.3$. The excentricity of the crack surface was changed by varying the angle θ in the range from $\theta = 0$ in the case with a planar circular crack in the solid to $\theta = 40°$. The surface of the spherical crack ($b = c$) was determined by the value $\theta = 30°$. As the problem is symmetric, each diagram shows the characteristics for both longitudinal and transverse reflected waves. It follows from Fig. 2 that an increase in the wavenumber leads to an increase in the amplitudes of scattering of waves of both modes. In the case of a planar crack, the wave field is symmetric about the equatorial plane, and the amplitudes (both F_P and F_{SV}) for directions I and II of the generating wave are equal to each other. The minimum values of the scattering amplitudes are observed in the equatorial plane; for F_{SV}, the minimum values are also observed for $\varphi = 0$ and π at the points where $F_{SV} = 0$. The maximums of the scattering amplitudes for longitudinal waves are located on the axis determining the direction of propagation of the generating wave; the corresponding maximums for transverse waves are located on the axes that form an angle close to 45° (depending on the wavenumber) with the previous direction. The absolute maximums of these parameters are reached on the convex side of the defect (see Fig. 1), and their values are higher in the case of diffraction of the external wave from this side. The difference in the crack response, depending on the two wave directions considered, is more pronounced in the range of high wavenumbers.

The data in Fig. 3 show that the amplitude of scattered waves decreases with increasing crack curvature. The reasons is a decrease in the specific elastic energy spent by the generating wave on defect opening. These results can be used as reference data in solving inverse problems of determining geometric parameters of the crack from scattered field data.

REFERENCES

1. V. M. Aleksandrov, B. I. Smetanin, and B. V. Sobol', *Thin Stress Concentrators in Elastic Solids* [in Russian], Fizmatlit, Moscow (1993).
2. V. V. Mykhas'kiv and I. O. Butrak, "Three-dimensional dynamic problems for an elastic solid with a gently sloping crack," *Fiz.-Khim. Mekh. Mater.*, **39**, No. 1, 69–78 (2003).

3. J. Dominguez and M. P. Ariza, “General BE approach for three-dimensional dynamic fracture analysis,” *Eng. Anal. Bound Elements*, **26**, No. 8, 639–651 (2002).
4. V. Z. Parton and V. G. Boriskovsky, *Dynamic Fracture Mechanics*, Hemisphere, New York (1989).
5. J. Sladek, V. Sladek, V. V. Mykhas’kiv, V. Z. Stankevych, “Application of mapping theory to boundary integral formulation of 3-D dynamic crack problems,” *Eng. Anal. Bound Elements*, **27**, No. 3, 203–213 (2003).
6. T. Tada, E. Fukuyama, and R. Madariaga, “Non-hypersingular boundary integral equations for 3-D non-planar crack dynamics,” *Comput. Mech.*, **25**, No. 6, 613–626 (2000).
7. Ch. Zhang and D. Gross, *On Wave Propagation in Elastic Solids with Cracks*, Comput. Mech. Publ., Southampton (1998).
8. T. N. Galishnikova and A. S. Il’inskii, *Numerical Methods in Diffraction Problems* [in Russian], Izd. Mosk. Univ., Moscow (1987).
9. E. V. Zakharov and I. V. Khaleeva, “Hypersingular integral equations of the 1st kind in problems of diffraction of electromagnetic waves from non-closed surfaces,” *Zh. Vychisl. Mat. Mat. Fiz.*, **33**, No. 2, 313–318 (1993).
10. A. V. Kaptsov and E. I. Shifrin, “Scattering of a normally incident longitudinal harmonic wave by a planar crack,” *Izv. Akad. Nauk SSSR, Mekh. Tverd. Tela*, No. 6, 106–112 (1986).
11. S. Hirose and J. D. Achenbach, “Higher harmonics in the far field due to dynamic crack-face contacting,” *J. Acoust. Soc. Amer.*, **93**, No. 1, 142–147 (1993).
12. J. D. Achenbach, “Quantitative nondestructive evaluation,” *Int. J. Solids Struct.*, **37**, No. 1, 13–27 (2000).
13. L. Yang and J. A. Turner, “Scattering of elastic waves in damaged media,” *J. Acoust. Soc. Amer.*, **113**, No. 6, 2992–3000 (2003).
14. V. V. Mykhas’kiv, “Boundary integral formulation of three-dimensional problems of steady vibrations of an infinite body with a crack located on an open Lyapunov surface,” *J. Math. Sci.*, **90**, No. 2, 1956–1960 (1998).
15. M. V. Khai, *Two-Dimensional Integral Equations of the Newton Potential Type and Their Applications* [in Russian], Naukova Dumka, Kiev (1993).